

# Gridpoint and spectral coupling of limited area model to a large scale model using simple 1d model

Martina Tudor

## ABSTRACT

Many research and operational forecasting applications are using limited-area models (LAM) that use higher resolutions and more advanced parameterizations of physical processes than global numerical weather prediction models, but suffer from one additional source of error - the lateral boundary conditions. The large scale model passes the information on its fields to LAM only over the narrow coupling zone at discrete times separated by a coupling interval of several hours. The LBC temporal resolution can be lower than the time necessary for a particular meteorological feature to cross the boundary. Although it should be defined according to the cross-boundary fluxes, it is usually determined by some non meteorological factors. A LAM user who depends on LBC data received from elsewhere or stored on storage of limited capacity can find that usual schemes for temporal interpolation of large scale data provide LBC data of unadequate quality.

The problem of a quickly moving cyclone that is not recognized by the operationally used gridpoint coupling scheme is examined using a simple one-dimensional model.

## 1 Introduction

Limited area models (LAMs) are used as an alternative to global numerical weather prediction (NWP) models for a wide variety of research and operational forecast applications. Particular LAM might suffer from different sources of forecast error: the parameterizations of physical processes, the initial conditions, the numerical algorithms and surface forcing. These also affect various global NWP models, but LAMs have one additional source of error related to their lateral boundary conditions (LBCs). an overview of the weaknesses of the LAM forecast caused by the LBCs was provided by Warner et al. (1997).

LBCs are obtained from models with coarser mesh in horizontal and vertical that usually use simpler (different) parameterizations of physical processes. Numerical procedures used on the interface of the two grids also generate error and the quality of the temporal interpolation of LBC data for LAM needs improvement (Termonia, 2003). Model error due to LBCs can be significant since it propagates into the domain interior during the forecast. It propagates and amplifies as it enters the domain of integration depending on the intensity of the cross-boundary flow and spreads further through the domain with longer time of integration. Complex orography, convection or cyclone at the boundary can produce inertia-gravity waves as well as differences in horizontal and vertical resolutions of the two grids.

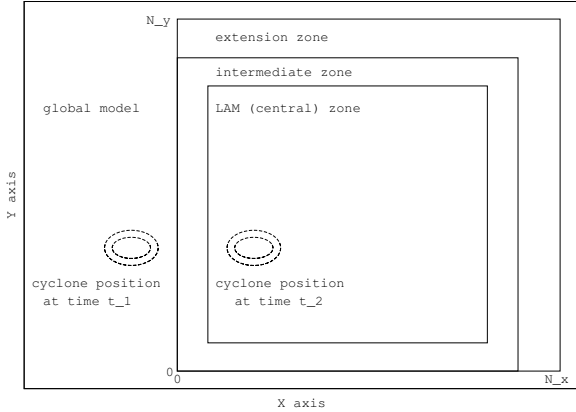


Figure 1: The geometry of the horizontal integration area for a spectral LAM that extends from 0 to  $N_x$  and from 0 to  $N_y$ . The time-dependent LBC fields are made bi-periodic by extending them into a zone outside the integration area (the extension zone). LAM solution is computed over the integration area and then relaxed to the LBC in the intermediate (relaxation) zone. A cyclone that crosses the boundary between two coupling times  $t_1$  and  $t_2$  is also shown.

The quality of the LBC data for operational as well as research purposes is severely restricted since its amount is limited by storage and data-transfer capacities. Large scale fields are usually available in temporal resolution of several hours, but they are needed at each LAM timestep which is usually on the order of several minutes. Consequently, LBCs are obtained at every LAM time-step using large scale fields that are interpolated in time. This interpolation procedure corrupts the fields, especially the features that have timescales shorter than the coupling interval. The situation can be made even worse when the large scale fields are taken only from the narrow area close to the domain lateral boundaries. Consequently, small scale features that are quick enough to enter the domain during one coupling interval are not suitably represented by the interpolated data.

The aim is to develop a simple coupling procedure that could be used operationally as a supplement or as an alternative to the Davies one either always, or when the quality of the LBCs is found insufficient by some diagnostic scheme (eg. Termonia, 2003). Different coupling procedures are implemented and tested using simple one-dimensional model.

The model is described in the following chapter. Results obtained using Davies scheme are presented in Section 3. The method of spectral coupling is described in Section 4 followed by its gridpoint counterpart in Section 5. The final part of this paper brings discussion and conclusions.

## 2 Model

A one dimensional spectral shallow-water model is used on a single horizontal level. It uses velocity and geopotential as model fields and it can run on global or limited area domains. It is integrated with two time level semi-implicit semi-Lagrangian scheme with a second order accurate treatment of the non-linear residual (Gospodinov, PhD).

A shallow-water spectral limited-area model that applies double Fourier spectral

representation on the model variables requires usage of time-dependent doubly periodic LBCs (Haugen and Machenhauer, 1993). Semi-implicit time integration and solving the Helmholtz equation in spectral space constrains the coupling procedure to be applied at the very beginning or end of the gridpoint computations (Radnoti, 1995). Another solution would be to develop a simple and cheap procedure that can be applied in the spectral space. The width of the extension zone is determined by the fact that the extended boundary fields should be well represented by the used truncation. The non-linear terms of the model equations are computed without aliasing if the number of gridpoints in the whole integration area is chosen so that  $N_x > 3M + 1$  and  $N_y > 3N + 1$  where  $(M, N)$  is the truncation wavenumber. Weak numerical diffusion is applied in spectral space at the end of the timestep to alleviate accumulation of energy at the smallest scales due to spectral blocking.

In the tests, the global model and LAM are using the same initial conditions that consist of a Gaussian shape depression that propagates from west to east with constant speed through the whole domain. This can be considered a simplified 1D version of the Christmats storm from 25th December 1999, even if the propagation speed in the 1D model is higher.

The global model run is on 200 gridpoints with  $\Delta x=40\text{km}$  and the LAM run is on 200 gridpoints, 11 of them are the extension zone on east and the 8 points on the eastern and western edge of the remaining 189 points are the relaxation zones. Both models use the same timestep of 150 seconds.

### 3 Gridpoint coupling

The flow-relaxation coupling scheme proposed by Davies (1976) relaxes the interior flow to the prescribed exterior flow consuming gravity wave energy and fine spatial scale potential vorticity near lateral boundaries representing adequately the outgoing gravity waves as well as geostrophical flow through the boundary. On lateral boundaries, the LAM is forced with large scale solution. The value of the model variable in the relaxation zone ( $X_C$ ) is computed from the large scale ( $X_{LS}$ ) and the small scale ( $X_{SS}$ ) values

$$X_C = \alpha X_{LS} + (1 - \alpha) X_{SS} \quad (1)$$

using the relaxation coefficient  $\alpha$

$$\alpha = (p + 1)Z^p - pZ^{p+1} \quad (2)$$

where  $Z = \frac{|x-x_e|}{x_e-x_e}$  is the relative distance of the gridpoint from the domain edge. The relaxation coefficient  $\alpha = 1$  in the extension zone and  $\alpha = 0$  in the central zone of LAM.

The large scale solution is known only at discrete times  $t_0, t_1, t_2, \dots$  where  $t_0$  is usually the initial time and the time difference between subsequent data is usually kept constant and referred to as coupling interval. The typical coupling interval in operational applications is 3 hours which is much longer than the typical timestep used in LAM (5-10 minutes). The large scale model state  $X_{LS}$  used in the relaxation zone is interpolated in time linearly:

$$X_{LS}(t) = w_1 X_{LS}^{t_1} + w_2 X_{LS}^{t_2} \quad \text{where} \quad w_1 = \frac{t_2 - t}{t_2 - t_1} \quad \text{and} \quad w_2 = \frac{t - t_1}{t_2 - t_1}$$

or quadratically

$$X_{LS}(t) = w_1 X_{LS}^{t_1} + w_2 X_{LS}^{t_2} + w_3 X_{LS}^{t_3} \quad \text{where} \quad w_1 = \frac{(t_2 - t)(t_3 - t)}{(t_2 - t_1)(t_3 - t_1)},$$

$$w_2 = \frac{(t_1 - t)(t_3 - t)}{(t_1 - t_2)(t_3 - t_2)} \quad \text{and} \quad w_3 = \frac{(t_1 - t)(t_2 - t)}{(t_1 - t_3)(t_2 - t_3)}$$

or using the tendency of the model state (Termonia, 2003)

$$X_{LS}(t) = w_1 X_{LS}^{t_1} + w_2 X_{LS}^{t_2} - w_1 w_2 (t_2 - t_1) \left[ \left( \frac{\partial X_{LS}}{\partial t} \right)^{t_2} - \left( \frac{\partial X_{LS}}{\partial t} \right)^{t_1} \right]$$

Another solution can be to increase the size of the coupling zone to include the area where the cyclone appears at the coupling interval.

Using gridpoint coupling with large scale data available with only 3 hourly interval allows for a cyclone to enter the domain area almost unnoticed (Figure 2). When the same computational scheme is used but with data available at every timestep, the disturbance is detected by the coupling scheme and further developed by LAM (Figure 3, left). This result represents our ideal goal of "perfect coupling" to be reached by the modified or new coupling scheme. Unfortunately, such perfect conditions of data availability are hardly ever met by LAM users, so other options are tested. Quadratic interpolation in time does not improve the results (not shown) while using the tendencies as well as values of the model variables with 3 hourly interval does improve the results (Figure 3, right) but unfortunately, this is still far from the desired ideal. When the LAM domain was shifted so that the cyclone minimum enters the domain at the moment when the large scale data are available, the cyclone was recognised, but its shape was distorted by the time interpolation of the large scale data (Figure 4, left). Another simple geometry solution would be to increase the size of the coupling zone. When its width was five-fold its usual (Figure 4, right) the cyclone was recognized, but it produced some spurious phenomena on its exit from the domain. These last two results show that there is an error inherent in the gridpoint coupling scheme since it misinterpretes or spoils the features that enter the domain giving more incentive for finding an alternative coupling scheme.

## 4 Spectral coupling

The spectral coupling scheme was built using similar mechanism as the Davies relaxation scheme. The boundaries are expressed in wavenumbers. Small wavenumber state is taken from the large scale, large wavenumber state is taken from LAM with a smooth transtion in between. The large scale spectral state is blended with the LAM. In other words, the large scale solution is spectrally filtered. The alternative coupling scheme was developed on a basis of a spectral model used with Fourier transform. A spectral method for nesting LAM in a larger scale model is implemented in the simple 1D model and tested.

### 4.1 The coupling method

For wavenumbers less than some treshold  $k_0$  we take spectral coefficients from the large scale model. For the wavenumbers lagrer than another treshold value  $k_1$ , spectral coef-

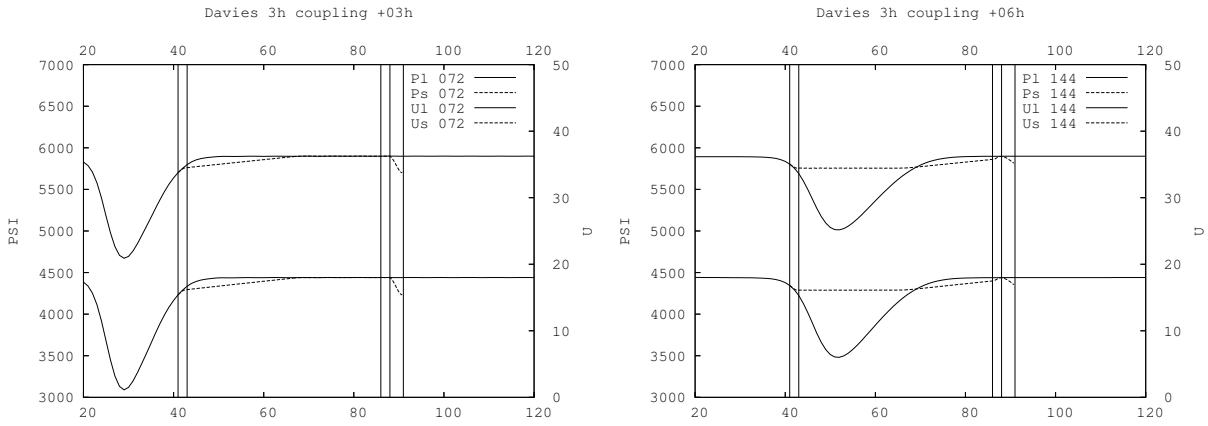


Figure 2: Results for coupling using Davies scheme with 3 hour interval between input large scale data, 3 hour forecast (left) and 6 hour forecast (right).

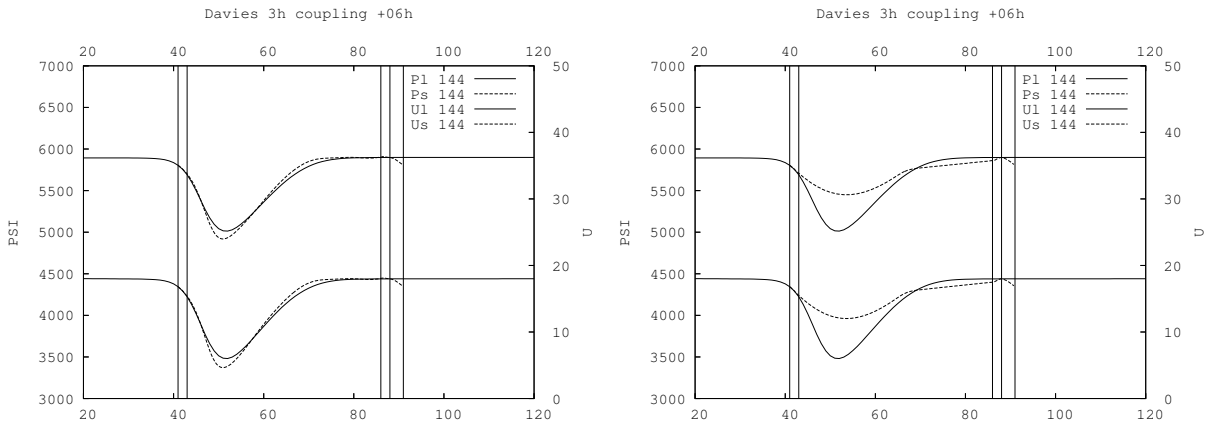


Figure 3: Results for coupling using Davies scheme with 1 time-step interval between input large scale data (left) and with 3 hour interval between input large scale data but using tendencies of the large scale fields for coupling (right). Both are 6 hour forecasts.

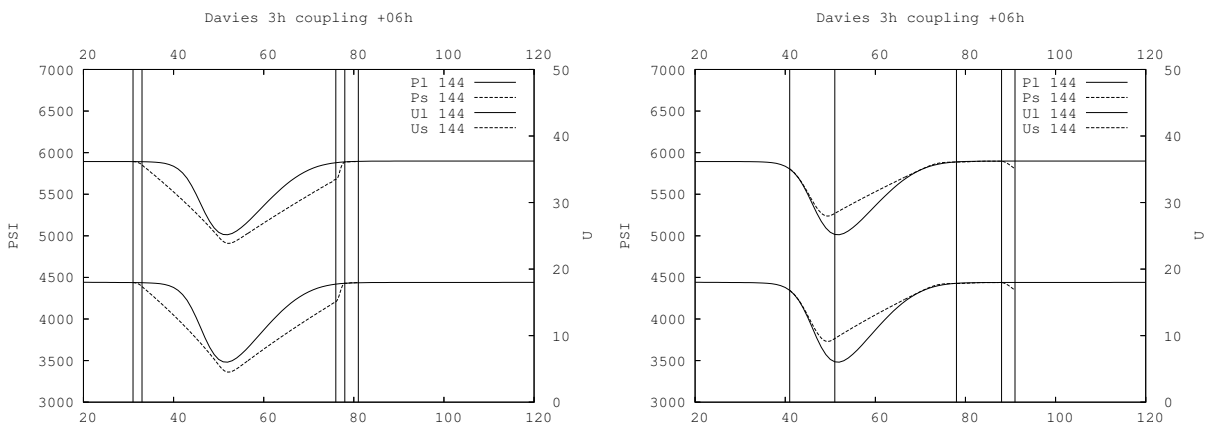


Figure 4: Results for coupling using Davies scheme with 3 hour interval between input large scale data and LAM domain shifted so that the cyclone enters the domain at the time large scale data are known (left) and when the coupling zone is increased 5 times: using 40 instead of 8 points (right).

ficients are taken from the LAM. The spectral coefficients for wavenumbers between  $k_0$  and  $k_1$  are computed

$$SP_C = \alpha SP_{LS} + (1 - \alpha) SP_{SS} \quad (3)$$

where the subscript  $C$  denotes the coupled values,  $LS$  denotes the values from global model or large scale LAM and  $SS$  denotes values from small scale or high resolution LAM. In analogy with the gridpoint (Davies) coupling scheme, the dependency of the  $\alpha$  coefficient on the wavenumber  $k$  can be linear

$$\alpha = \frac{k_1 - k}{k_1 - k_0} \quad (4)$$

or have a polynomial dependence on  $k$

$$\alpha = (p + 1)z^p - pz^{p+1} \quad \text{for } p > 0 \quad (5)$$

$$\alpha = 1 - (-p + 1)(1 - z)^{-p} - pz^{-p+1} \quad \text{for } p < 0 \quad (6)$$

where  $z = \frac{k_1 - k}{k_1 - k_0}$  is the relative distance of the wavenumber  $k$  from the small scale wavenumber  $k_1$  and  $p$  is the order of the polynome. The polynomial dependence of  $\alpha$  on wavenumber did not bring much improvement over the linear one in the tests using the simple one dimensional model, so the linear dependence will be kept in the following experiments.

The spectral coupling scheme is scale selective, the large scales are dominated by the spectra of the large scale model and only small scales are dominated by the LAM. Its advantage is that the large scale solution is forced to LAM on the whole domain area. Unfortunately, spectral coupling scheme alone cannot eliminate spurious wave propagation from the lateral boundaries inward. All the waves that exit on one side of the domain freely enter on the opposite side. This is why we still need to use the Davies scheme simultaneously to provide the damping on the domain edges. In other words, both coupling methods are combined.

The relaxation takes place at the end of the gridpoint computations simultaneously with the Davies relaxation scheme, but it could be used in spectral space.

## 4.2 Coupling without interpolation of large scale fields in time

The large scale fields are known only at discrete time intervals. In the gridpoint coupling scheme the coupling is done every timestep and the large scale fields on the boundaries are interpolated in time. Spectral coupling could be done only at the coupling steps, when the large scale data are available, or more often up to every LAM timestep.

First we tested several options of introducing large scale data into LAM without being interpolated in time. If the LAM solution is forced by the large scale one only at the coupling steps, the cyclone appears suddenly, during one timestep. Such result suggests that this method is not good for a real LAM with more sophisticated dynamics and physics

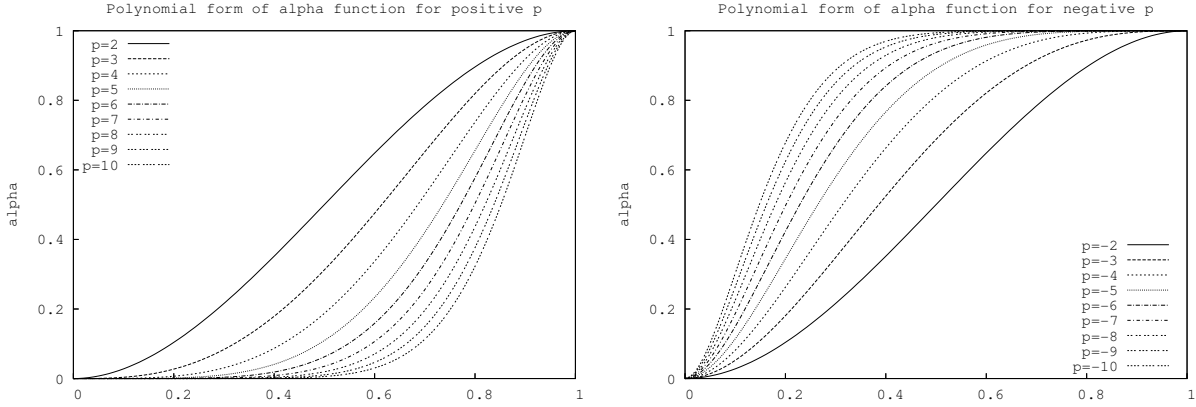


Figure 5: Polynomial forms of alpha function defined for the relative distance from the small scale wave number for the case when  $k_0 = 2$ ,  $k_1 = 8$ , for positive values of  $p$  (left) and negative values of  $p$  (right).

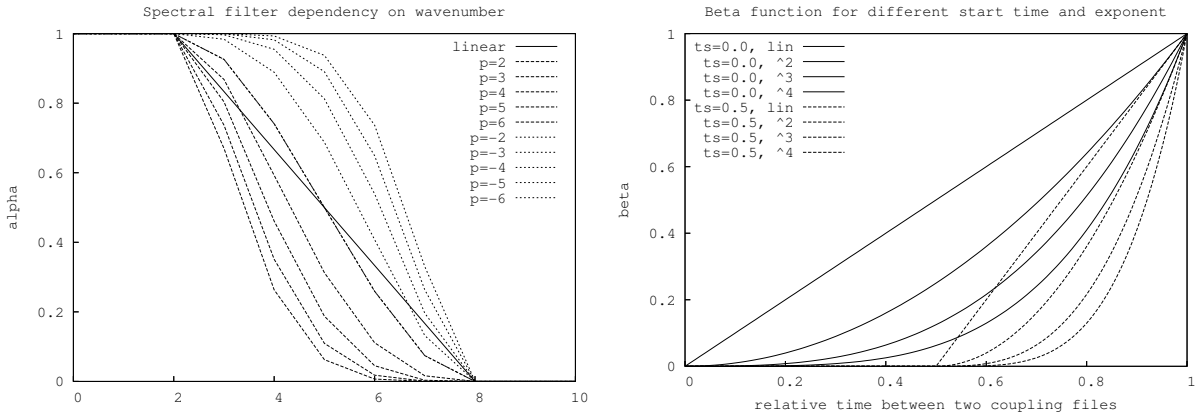


Figure 6: The spectral filter (alpha) dependence on the wavenumber for linear and polynomial functions (left) and dependence of the  $\beta$  function on the relative position in time between the two coupling files (right).

parameterization package.

Instead of introducing large scale data suddenly, in one timestep, an attempt was made to introduce it gradually during the coupling interval, so that coupling coefficient  $\alpha$  was multiplied by a time dependent  $\beta$  function

$$\beta = \left( \max\left[0, \frac{1}{1-t_s} \left( \frac{t-t_1}{t_2-t_1} - t_s \right) \right] \right) \quad (7)$$

where  $t_s$  is the timestep when the large scale solution from the second coupling time starts to be used,  $t_1$  is the time of the first coupling file,  $t_2$  is the time of the second coupling file. The time  $t$  is from the interval  $t_1 < t < t_2$ . This way the large scale data are not interpolated in time, but the data from the second coupling step are gradually introduced to the model during the coupling interval.

Unfortunately, such method leads to unphysical solution of a false rapid cyclogenesis that develops in the domain, not an undisturbed transfer of a cyclone into the model

domain. Therefore, we need to accomplish a different type of smooth transition between the coupling steps when the large scale data are known that would allow more physical representation of the model evolution on the lateral boundaries.

### 4.3 Temporal interpolation of spectral coefficients

The spectral coefficients of the large scale fields are interpolated in time before being used by the coupling procedure. In analogy with the gridpoint coupling procedure, this interpolation can be linear or quadratic in time and it can use tendencies of the spectral coefficients. We use similar formulas as for gridpoint coupling when the values of the model fields are replaced by its spectral coefficients.

Results for linear interpolation of spectral coefficients in time is shown in Figure 7. Instead of advection of the cyclone, a dipole is obtained. The cyclone develops and then dissolves only to develop on another position simultaneously. Similar results were obtained for quadratic interpolation of spectral coefficients in time as well as when their tendencies (acceleration) were used (not shown). Since interpolation spectral coefficients in time also led to unrealistic model behaviour, so an attempt was made using amplitude and phase of spectral components.

### 4.4 Temporal interpolation of amplitude and phase of spectral coefficients

Amplitude and phase are first computed from the spectral components and then interpolated in time, either linearly or quadratically, using acceleration, tendencies, the integrated tendencies or polynomial interpolation. The interpolated amplitude and phase are used to compute the large scale spectral components used for coupling at a given timestep. Linear and quadratic time interpolation of amplitude and phase is done using same formulas as in gridpoint coupling schemes and acceleration is accounted for in analogous way. The resulting model run showed significant improvements compared to the run when spectral coefficients were interpolated. The cyclone was mostly advected and the dipole problem almost disappeared. This result encouraged searching for alternative schemes for interpolation of amplitude and phase in time.

#### 4.4.1 Average of extrapolated values

Alternative time interpolating scheme has been introduced that estimates the value of the model variable  $X$  at time  $t$  by extrapolating it from the coupling steps. Assume that model variable  $X$  at one coupling step at time  $t_1$  has known value  $X_1$  and a time derivative  $\left(\frac{\partial X}{\partial t}\right)_{t_1}$  and in the next coupling step at time  $t_2$  has value  $X_2$  and derivative  $\left(\frac{\partial X}{\partial t}\right)_{t_2}$ . The simplest way of accounting for the tendency in the interpolation scheme is to compute the forward extrapolated value from time  $t_1$

$$X_1(t) = X_1 + \left(\frac{\partial X}{\partial t}\right)_{t_1} (t - t_1)$$

and backward extrapolated value from time  $t_2$

$$X_2(t) = X_2 + \left( \frac{\partial X}{\partial t} \right)_{t_2} (t - t_2)$$

and finally compute their weighted average

$$X(t) = w_1 X_1(t) + w_2 X_2(t)$$

Usage of this interpolating scheme allows the cyclone to smoothly enter the domain, to be advected through it and exit (Figure 8). Unfortunately, there are few spurious waves generated on top of the simulated cyclone that spoil the solution slightly. Other nuisance is that the LAM contribution to the resulting model evolution is suppressed by the spectral nudging of the spectral components towards the large scale solution. In other words, LAM does not bring useful contribution to the evolution of the model variables or this contribution is hidden with spurious waves that are consequence of the temporal interpolation of the large scale fields.

#### 4.4.2 Integrated weighted tendencies

Instead of using fixed value for the tendency for the whole  $(t - t_1)$  or  $(t_2 - t)$  period, we can use a weighted average of the two tendencies at each time step and then compute the integral from  $t_1$  to  $t$  or from  $t$  to  $t_2$  respectively.

Value of the model variable  $X$  at time  $t$  can be estimated by forward integration of the following expression

$$X_1(t) = X_1 + \int_{t_1}^t \left( w_1 \left( \frac{\partial X}{\partial t} \right)_{t_1} + w_2 \left( \frac{\partial X}{\partial t} \right)_{t_2} \right) dt$$

where  $w_1 = \frac{t_2 - t}{t_2 - t_1}$  and  $w_2 = \frac{t - t_1}{t_2 - t_1}$  are functions of time  $t$ . The obtained function of time is

$$X_1(t) = X_1 + \left( \frac{\partial X}{\partial t} \right)_{t_1} (t - t_1) + \frac{1}{2} \left( \left( \frac{\partial X}{\partial t} \right)_{t_2} - \left( \frac{\partial X}{\partial t} \right)_{t_1} \right) \frac{(t - t_1)^2}{t_2 - t_1}$$

or alternatively, similar expression can be obtained when integrating from time  $t_2$  backward

$$X_2(t) = X_2 - \int_t^{t_2} \left( w_1 \left( \frac{\partial X}{\partial t} \right)_{t_1} + w_2 \left( \frac{\partial X}{\partial t} \right)_{t_2} \right) dt$$

yielding alternative function of time

$$X_2(t) = X_2 - \left( \frac{\partial X}{\partial t} \right)_{t_2} (t_2 - t) + \frac{1}{2} \left( \left( \frac{\partial X}{\partial t} \right)_{t_2} - \left( \frac{\partial X}{\partial t} \right)_{t_1} \right) \frac{(t_2 - t)^2}{t_2 - t_1}.$$

The final interpolation function is the linear combination of the two

$$X(t) = w_1 X_1(t) + w_2 X_2(t)$$

This interpolation scheme does not generate spurious waves (Figure 9) and apparently there is some benefit of the higher resolution LAM run since it contributes to the evolution of the disturbance.

### 4.4.3 Polynomial interpolation

Alternative interpolation function can be computed using the values of the model variable  $X$  and its derivative at times  $t_1$  and  $t_2$  to evaluate coefficients in a 3rd order polynome. First assume a polynomial dependence of the variable  $X$  in time:

$$X(t) = a + bt + ct^2 + dt^3$$

and compute the coefficients assuming  $t_1 = 0$  for simplicity

$$\begin{aligned} a &= X(t = 0) = X_1 \\ b &= \left( \frac{dX}{dt} \right)_{t=0} = \left( \frac{\partial X}{\partial t} \right)_{t_1} \\ c &= \frac{3}{t_2^2} \left[ X_2 - X_1 - \frac{1}{3} \left( 2 \left( \frac{\partial X}{\partial t} \right)_{t_1} + \left( \frac{\partial X}{\partial t} \right)_{t_2} \right) t_2 \right] \\ d &= -\frac{2}{t_2^3} \left[ X_2 - X_1 - \left( \left( \frac{\partial X}{\partial t} \right)_{t_1} + \left( \frac{\partial X}{\partial t} \right)_{t_2} \right) t_2 \right] \end{aligned}$$

This interpolation scheme also allows for the cyclone to smoothly enter the domain, but unfortunately it also amplifies some scales more than it should so spurious waves appear in the LAM solution (figure not shown, results qualitatively similar to those in Figure 8).

Spectral coupling procedure using temporal interpolation of amplitude and phase instead of spectral coefficients has reproduced the model evolution in more physical way yielding results that are similar to the test with gridpoint coupling using large scale data from each timestep - the "perfect coupling" test (Figure 3, left). Spectral coupling alone allows for waves to re-enter the domain upon exiting on the opposite side due to biperiodization of the lage scale fields. Therefore it still requires simultaneous usage of the gridpoint coupling procedure on the domain edges to filter the waves that would iotherwise re-ener the domain.

Unfortunately, the temporal interpolation scheme might generate spurious waves that could spoil the solution or mask the LAM contribution to the model evolution. It is also possible that these spurious waves are partly i a consequence of double coupling on the domain edges where the spectral coupling procedure could push the model fields in different way than the gridpoint procedure. Therefore another alternative that could potentially allow for physical evolution of LBC conditions and enable evolution of the LAM solution in the central part of the domain undisturbed by the spectral nudging toward the large scale data.

## 5 Gridpoint coupling with phase

The model state  $X_{LS}$  is transformed from gridpoint to the spectral space, and the spectral coefficients are obtained. Then the amplitude and the phase angle of the complex spectral coefficients are computed and interpolated in time as when doing the spectral coupling.

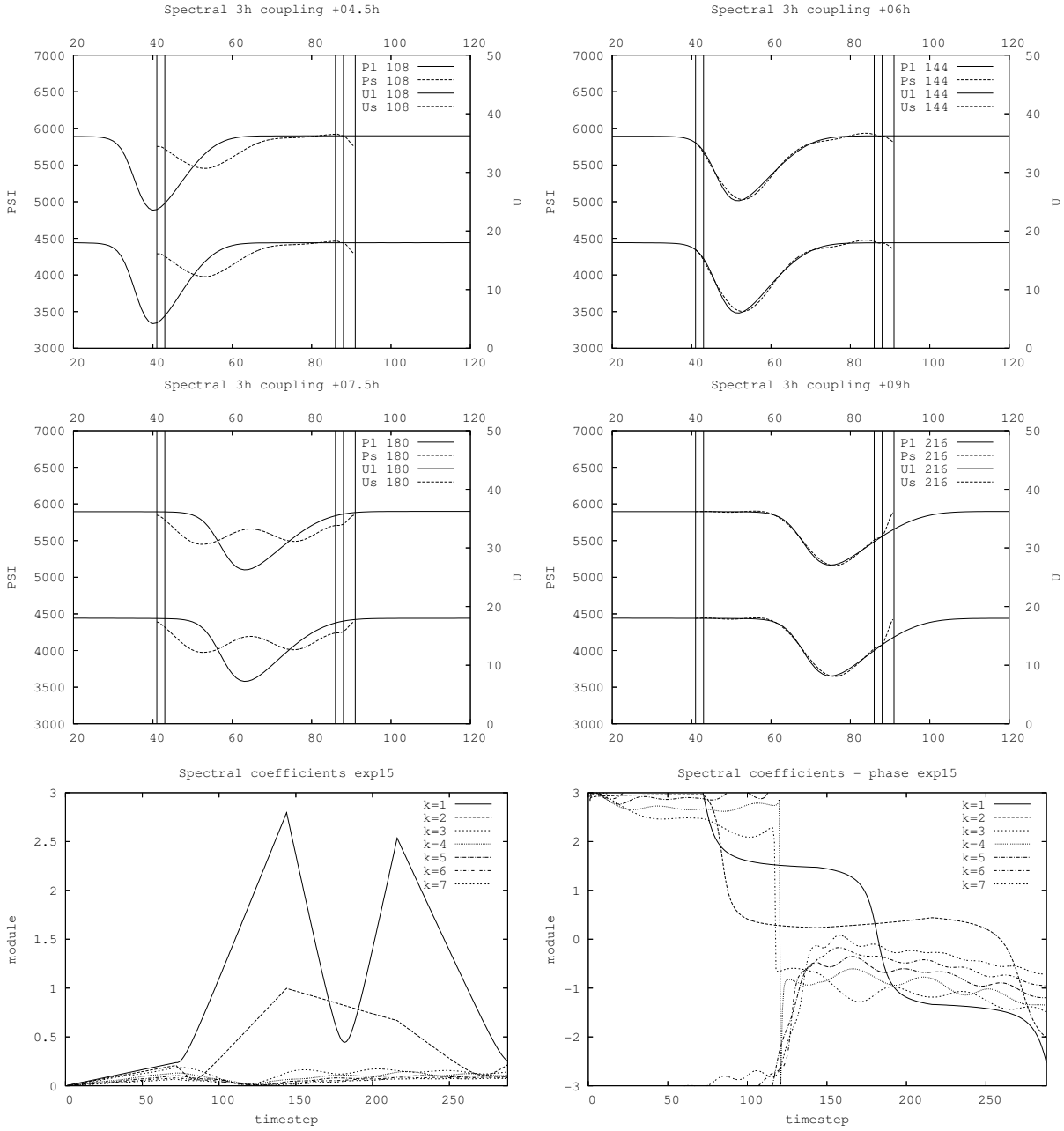


Figure 7: Results using spectral coupling scheme with 3 hour interval between input large scale data, when the spectral coefficients are interpolated linearly in time, after 4.5 (a), 6 (b), 7.5 (c), 9 (d), hours of integration, and evolution of amplitude (e) and phase (f) of the first 7 spectral components during the integration.

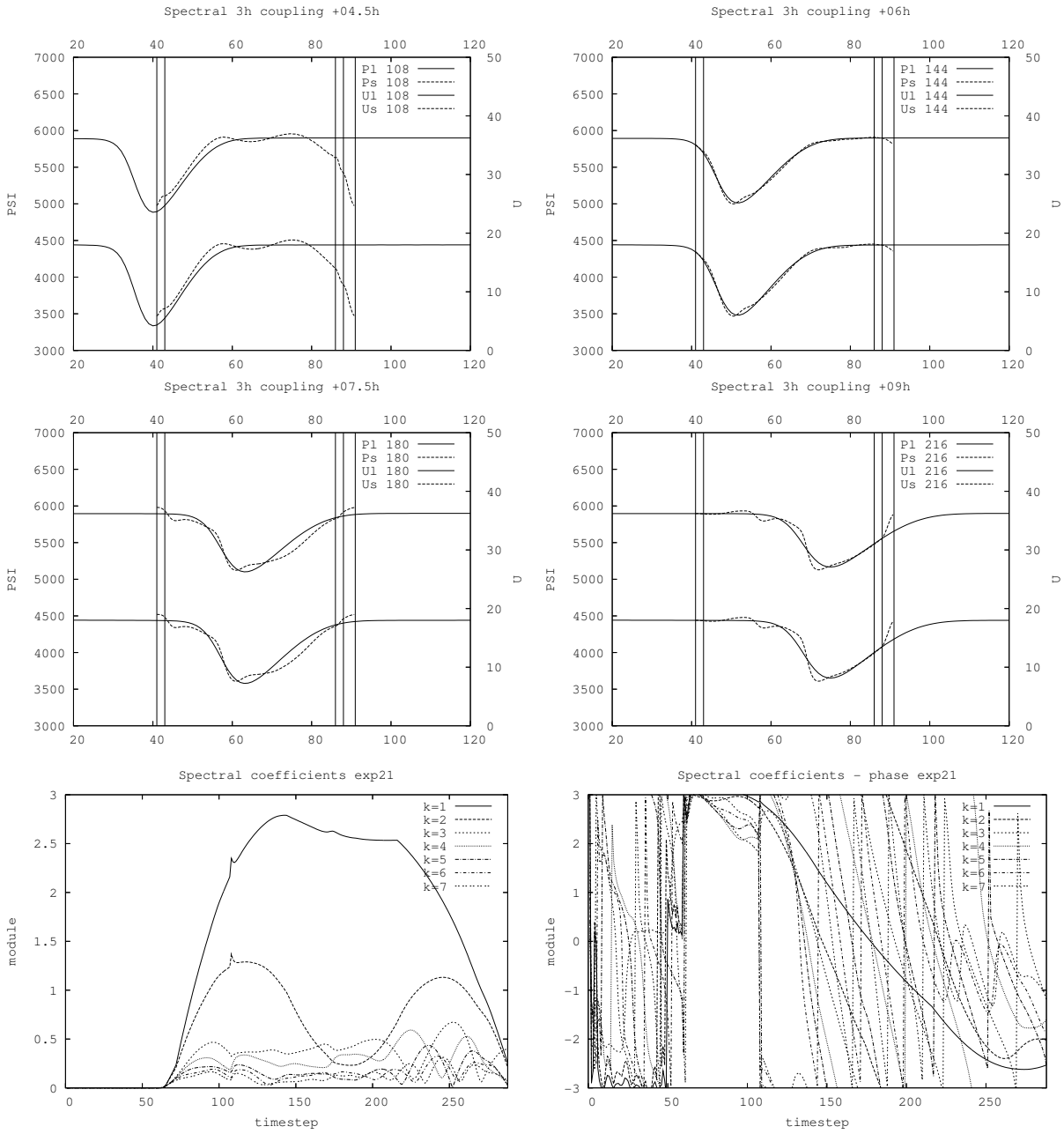


Figure 8: Results using spectral coupling scheme with 3 hour interval between input large scale data when amplitude and phase are interpolated in time using the extrapolated values, after 4.5 (a), 6 (b), 7.5 (c), 9 (d), hours of integration, and evolution of amplitude (e) and phase (f) of the first 7 spectral components during the integration.

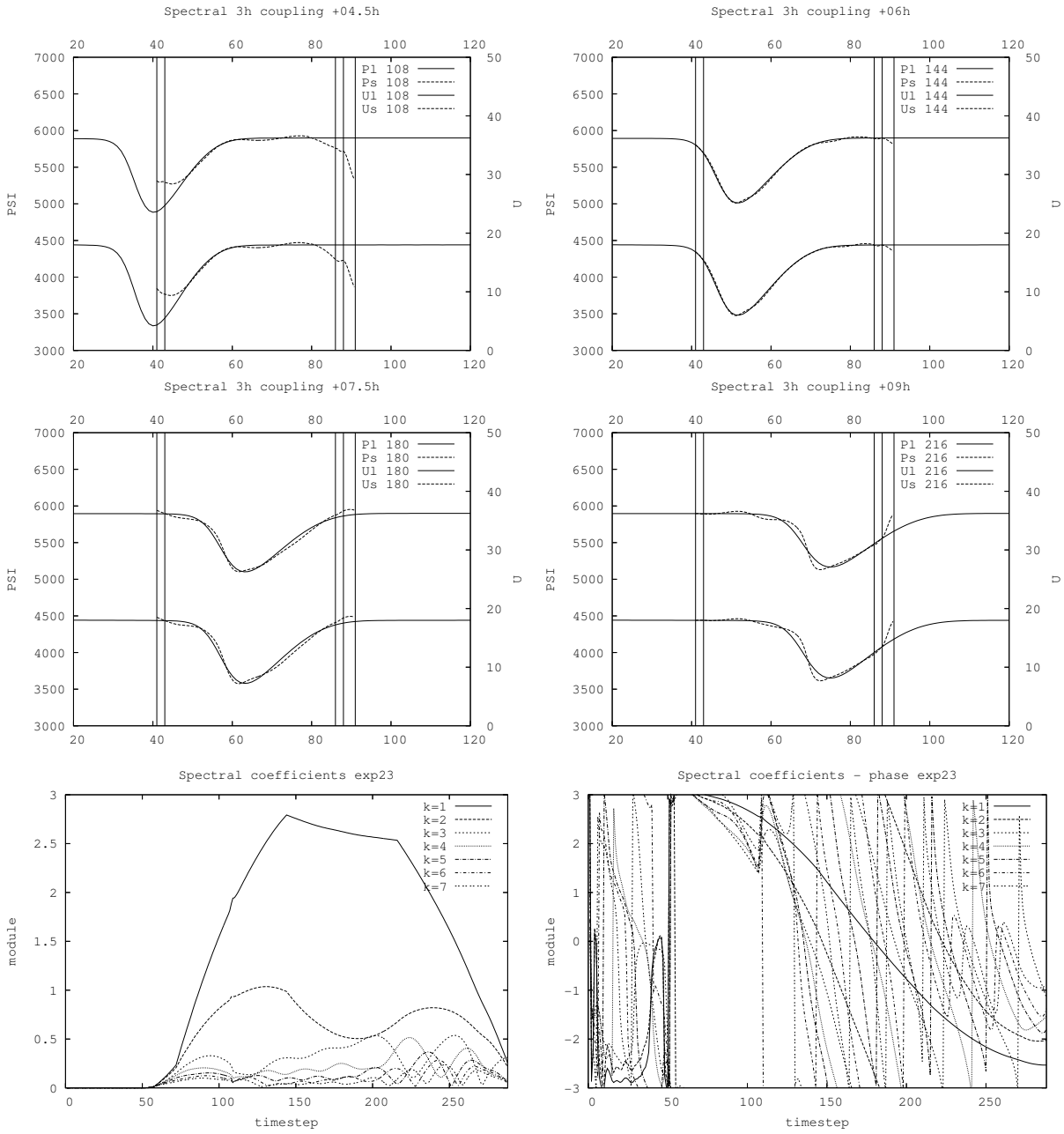


Figure 9: Results using spectral coupling scheme with 3 hour interval between input large scale data when amplitude and phase are interpolated in time using the integrated values, after 4.5 (a), 6 (b), 7.5 (c), 9 (d), hours of integration, and evolution of amplitude (e) and phase (f) of the first 7 spectral components during the integration.

The interpolated amplitude and phase angle are used to compute the interpolated spectral coefficients which are transformed back from spectral to gridpoint space. This way we obtain the large scale fields used for gridpoint coupling.

The time interpolation of amplitude and phase can also be linear or quadratic, use tendencies for integral or polynomial interpolation. When the amplitude and phase are interpolated linearly in time, the simulated cyclone is significantly weaker than with the perfect coupling scheme, but recognized. Unfortunately it is followed by a strong false anticyclone (not shown). Results are very similar with quadratic coupling. When the acceleration of amplitude and phase is used, the simulated cyclone is stronger and false anticyclone is reduced. Using average of extrapolated values gives satisfactory depth of the cyclone but the amplitude of few short modes is a bit too strong (Figure 10). Other results using tendencies of the model fields, either integrated between coupling steps or using polynomial interpolation give similar results as the simplest case mentioned previously. Cyclone smoothly enters the domain, although less deep than in the large scale model. But since this scheme relaxes the LAM solution to the large scale one only in the narrow area close to the domain edge, LAM can contribute to the development of the disturbance. Unfortunately, some of the benefit of the gridpoint coupling is lost since the longest modes also re-enter the domain, although much weaker, leaving the remaining wave. This is a consequence of the biperiodization of the large scale fields.

## 6 Conclusions

Gridpoint coupling using standard Davies scheme on a narrow area close to the edges of the LAM domain with a coupling interval of several hours mixes a signal that enters the domain. Two possible alternatives are presented, one does the coupling in the spectral space, while the other only interpolates the large scale fields in time in spectral space but does the coupling in gridpoint space. Both of them are able to represent this signal in LBC. Unfortunately, they suffer supporting some spurious waves that could re-enter the domain as a consequence of biperiodization. These waves can be filtered by the gridpoint coupling scheme.

Both schemes could be used either always or only when some diagnostic procedure detects that some signal has entered the LAM domain without being detected by the LBC procedure.

## 7 References

Davies, H.C., 1976: A lateral boundary formulation for multi-level prediction models. *Quart. J. Roy. Meteor. Soc.*, 102, 405-418.

Davies, H.C., 1983: Limitations of some common lateral boundary schemes used in regional NWP models. *Mon. Wea. Rev.*, 111, 1002-1012.

Haugen, J.E., and B. Machenhauer, 1993: A spectral limited-area formulation with time-dependent boundary conditions applied to the shallow-water equations. *Mon. Wea.*

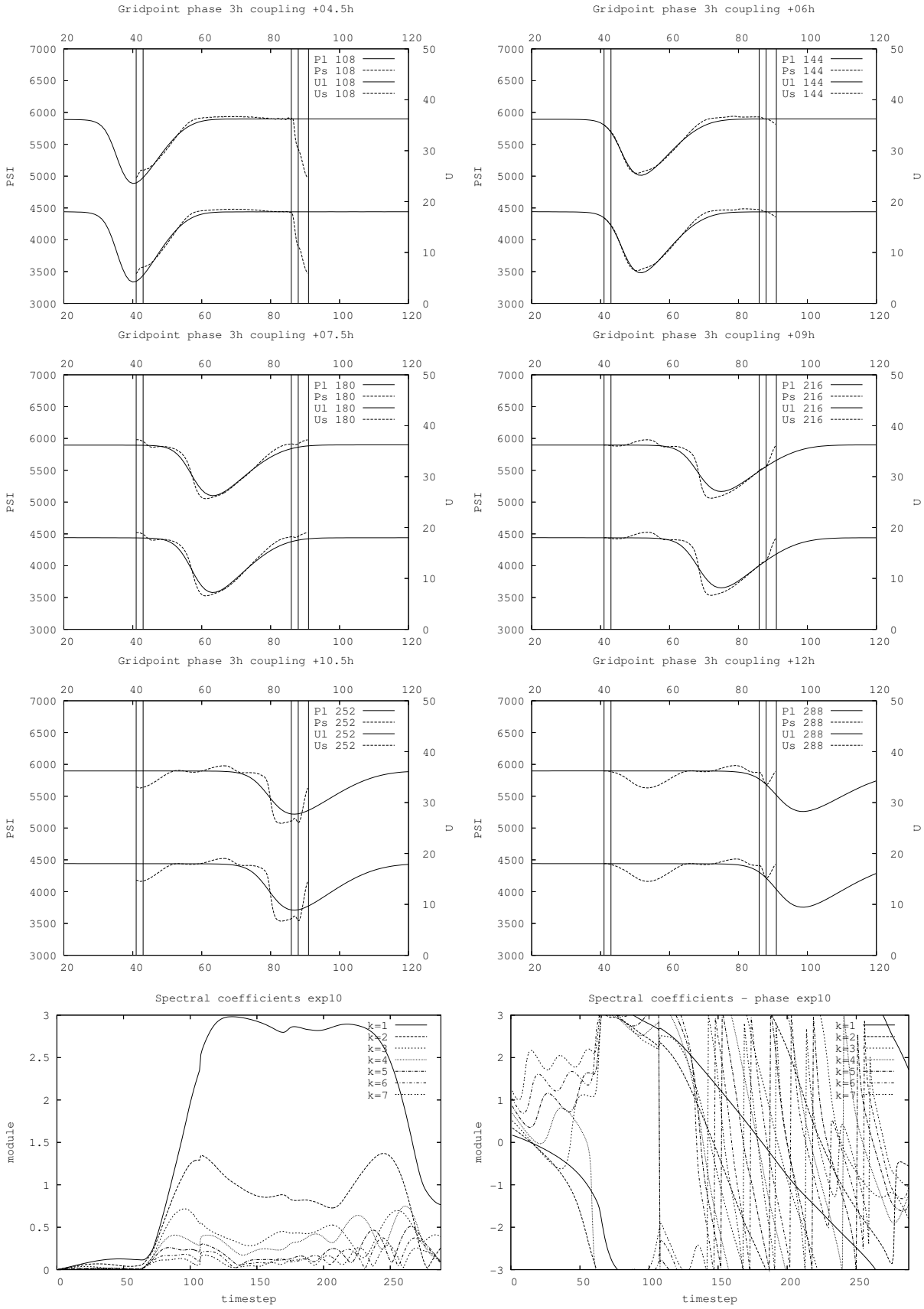


Figure 10: Results for coupling using gridpoint scheme with 3 hour interval between input large scale data when the phase angle method is used in the relaxation zone, after 4.5 (a), 6 (b), 7.5 (c), 9 (d), 10.5 (e) and 12 (f) hours of integration, and evolution of amplitude (g) and phase (h) of the first 7 spectral components during the integration.

Rev., 121, 2618-2630.

Radnóti, G., 1995: Comments on "A spectral limited-area formulation with time-dependent boundary conditions applied to the shallow-water equations." *Mon. Wea. Rev.*, 123, 3122-3123.

Termonia, P., 2003: Monitoring and improving the temporal interpolation of lateral-boundary coupling data for limited area models. *Mon. Wea. Rev.*, 131, 2450-2463.

Termonia, P., 2004: Monitoring of the coupling update frequency of a limited-area model by means of a recursive digital filter. *Mon. Wea. Rev.*, 132, 2130-2141.

Warner, T.T., R.A. Peterson and R.E. Treadon, 1997: A tutorial on lateral boundary conditions as a basic and potentially serious limitation to regional numerical weather prediction. *Bull. Amer. Meteor. Soc.*, 78, 2599-2617.

## 8 Appendix A - Fourier transform and computation of amplitude and phase from spectral coefficients

$$X_j = \sum_{k=0}^{N-1} c_k e^{i2kj\frac{\pi}{N}}$$

where  $c_k = a_k + ib_k = r_k e^{i\varphi}$ ,  $c_{N-k} = a_k - ib_k$ . The complex coefficients are computed using forward fast Fourier transform (FFT)

$$a_k = \frac{1}{N} \sum_{j=0}^{N-1} X_j \cos(2kj\frac{\pi}{N})$$

$$b_k = -\frac{1}{N} \sum_{j=0}^{N-1} X_j \sin(2kj\frac{\pi}{N})$$

The amplitude and the phase angle are computed from the complex spectral coefficients

$$r_k = (a_k^2 + b_k^2)^{\frac{1}{2}}$$

$$\varphi_k = \begin{cases} \arccos\left(\frac{a_k}{\sqrt{a_k^2 + b_k^2}}\right) & \text{if } b_k > 0 \\ -\arccos\left(\frac{a_k}{\sqrt{a_k^2 + b_k^2}}\right) & \text{if } b_k < 0 \end{cases}$$

and interpolated in time

$$r_k = \frac{t_2 - t}{t_2 - t_1} r_k^{t_1} + \frac{t - t_1}{t_2 - t_1} r_k^{t_2}$$

$$\varphi_k = \frac{t_2 - t}{t_2 - t_1} \varphi_k^{t_1} + \frac{t - t_1}{t_2 - t_1} \varphi_k^{t_2}$$

the spectral coefficients are computed from the new values of amplitude and the phase angle

$$a_k + ib_k = r_k e^{i\varphi_k}$$

and transferred back from spectral to physical space to obtain the new large scale field used in coupling.